Domain Wall Creation in Nanostructures Driven by a Spin-Polarized Current

D. Ravelosona, S. Mangin, Y. Lemaho, J. A. Katine, B. D. Terris, Eric E. Fullerton

▶ **To cite this version:**

D. Ravelosona, S. Mangin, Y. Lemaho, J. A. Katine, B. D. Terris, et al.. Domain Wall Creation in Nanostructures Driven by a Spin-Polarized Current. Physical Review Letters, 2006, 96 (18), pp.186604. 10.1103/PhysRevLett.96.186604 . hal-02086094

HAL Id: hal-02086094
https://hal.univ-lorraine.fr/hal-02086094v1

Submitted on 1 Apr 2019

HAL is a multi-disciplinary open access archive for the deposit and dissemination of scientific research documents, whether they are published or not. The documents may come from teaching and research institutions in France or abroad, or from public or private research centers.

L'archive ouverte pluridisciplinaire **HAL**, est destinée au dépôt et à la diffusion de documents scientifiques de niveau recherche, publiés ou non, émanant des établissements d'enseignement et de recherche français ou étrangers, des laboratoires publics ou privés.

Domain Wall Creation in Nanostructures Driven by a Spin-Polarized Current

D. Ravelosona,[1,2] S. Mangin,[1,3] Y. Lemaho,[1,2] J. A. Katine,[1] B. D. Terris,[1] and Eric E. Fullerton[1]

[1]*Hitachi Global Storage Technologies, San Jose Research Center, 650 Harry Road, San Jose, California 95120, USA*

[2]*Institut d'Electronique Fondamentale, UMR CNRS 8622, Université Paris Sud, 91405 Orsay Cedex, France*

[3]*LPM, U.H.P-Nancy I, B.P. 239 F-54506 Vandoeuvre cedex, France*

(Received 23 February 2006; published 10 May 2006)

We report on current-driven magnetization reversal in nanopillars with elements having perpendicular magnetic anisotropy. Whereas only the two uniform magnetization states are available under the action of a magnetic field, we observed current-induced Bloch domain walls in pillars as small as 50×100 nm^2. This domain wall state can be further controlled by current to restore the uniform states. The ability to nucleate and manipulate domain walls by a current gives insight into the reversal mechanisms of small nanoelements and provides new prospects for ultrahigh density spintronic devices.

DOI: 10.1103/PhysRevLett.96.186604 PACS numbers: 72.25.−b, 75.60.Ch, 75.60.Jk, 85.75.−d

A key aspect of magnetic nanostructures is the study and control of their domain structure. For many applications, such as spin valve read heads, great care is taken to avoid the creation of domains or the presence of domain wall motion within the magnetic layers. In other devices, the controlled motion of domain walls (DWs) is thought to enable new applications such as alternative magnetic memories or programmable logic devices [1,2]. The observation of magnetization reversal of nanoelements driven by polarized spin currents provides new opportunities to study and control domain structures. It should be possible, by the judicious use of both spin currents and applied magnetic fields, to separate the nucleation and propagation processes of domain walls during reversal in magnetic nanostructures in a way that is not possible using only an applied field.

Very recent theoretical models [3,4] have pointed out that an in-plane spin current can break the uniform magnetization state of a wire into a multiple domain structures. However, this is believed to occur for unrealistically high current densities (10^8–10^{10} A/cm^2). A more efficient approach to current-induced domain nucleation is to have a spin-polarized current flow perpendicular to the plane (CPP) of the film in nanopillars. Indeed, both experimental evidence of inhomogeneous switching [5–9] and micromagnetic calculations [10,11] for in-plane magnetized CPP nanoelements have suggested the formation of complex domain structures under relatively low current densities. Although nonuniform magnetization configurations such as vortex, *S*, or *C* states may be induced, well-defined DWs are unlikely to be created for in-plane magnetized nanopillars because the typical Néel wall width (>100 nm) is on the same scale as the device.

In this Letter, we describe domain nucleation and controlled domain wall propagation in magnetic elements as small as 50×100 nm^2. This is achieved using high coercivity films with perpendicular magnetic anisotropy that support Bloch walls on the order of 10 nm in width. We find that domains can be nucleated with modest CPP current densities of 10^7 A/cm^2, and the relatively high DW pinning force, strong dipolar fields in the perpendicular geometry, and possible effects of current redistribution can stabilize the resulting DW. This DW state is found to be stable over a quite large region of the current-field phase diagram, and the two uniform magnetization states can be restored by either applied field and/or current. In addition to the current-driven control of DW nucleation, this study clearly demonstrates that the macrospin model [12] is not fully suitable to characterize the reversal processes in films with perpendicular anisotropy even for very small nanoelements.

The structures used in this study are spin valves based on Co/Ni multilayers with perpendicular magnetic anisotropy (for details, see the methods section in Ref. [13]). They consist of SiN/Ta(5 nm)/Cu(35 nm)/Pt(3 nm)/reference layer/Cu(4 nm)/free layer/Pt(3 nm)/Cu(15 nm)/Ta(5 nm) as shown schematically in Fig. 1(a). The reference layer consists of a composite of Co/Pt and Co/Ni multilayers $[\mathrm{Co}(2.5\ \text{Å})/\mathrm{Pt}(5.2\ \text{Å})]_4/\mathrm{Co}(2.5\ \text{Å})/\mathrm{Co}(1\ \text{Å})/\mathrm{Ni}(6\ \text{Å})]_4/\mathrm{Co}(1\ \text{Å})$ to enhance the perpendicular anisotropy, and the free layer is a $[\mathrm{Co}(1\ \text{Å})/\mathrm{Ni}(6\ \text{Å})]_4/\mathrm{Co}(1\ \text{Å})$ multilayer. We find that use of Co/Ni magnetic multilayers provides perpendicular anisotropy with higher giant magnetoresistance (GMR) ratios and spin-torque efficiencies when compared to Co/Pt multilayers. This is most likely the result of the high spin-orbit scattering of the weakly or nonmagnetic Pt layers in Co/Pt multilayers. CPP-GMR hexagonal shaped nanopillars were fabricated by electron beam lithography and ion beam milling. The differential resistance was measured using a high sensitivity ac ($\sim 10\ \mu$A) Wheatstone bridge and the dc current injected using a bias *T*. For all the experiments, the reference layer pointed down as shown in Fig. 1(a).

Figure 1(b) shows the differential resistance dV/dI as a function of the net perpendicular field (H_{net}) for a 100×200 nm^2 nanopillar. The curves correspond to the switching of the free layer from the antiparallel (AP) to parallel (P) states for a dc current $I = 0$ and $I = -7$ mA ($\sim 4 \times 10^7$ A/cm^2). For $I = 0$, we observe a discrete reversal of the free layer at the coercive field of $H_{\mathrm{net}} = -3.1$ kOe.

 © 2006 The American Physical Society

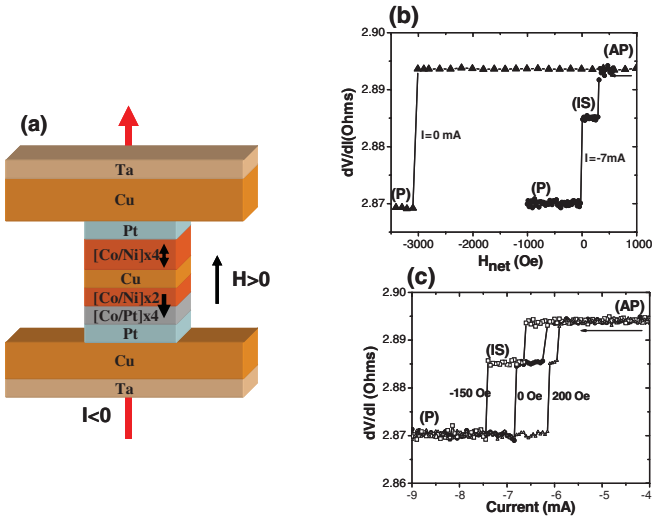

FIG. 1 (color). (a) Schematic of the nanopillars used in this experiment. A negative current corresponds to electron flowing from the bottom to the top electrodes. (b) Differential resistance as a function of net perpendicular magnetic field at $I = 0$ and $I = -7$ mA for a 100×200 nm^2 pillar. (c) Differential resistance as a function of current at $H_{\text{net}} = -150$, 0, and 200 for a 100×200 nm^2 pillar. The initial state is the AP state.

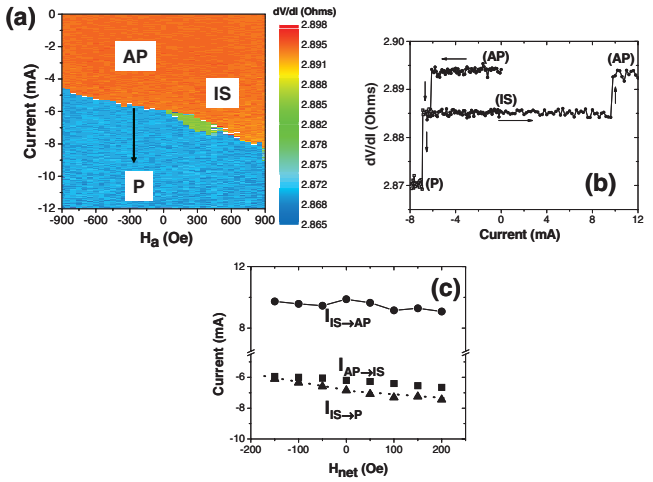

FIG. 2 (color). (a) Current-field phase diagram of dV/dI for a 100×200 nm^2 pillar realized by measuring dV/dI while sweeping the current from 0 to -12 mA in steps of 50 μA at constant magnetic field H_a that is stepped by 50 Oe for each scan. The initial state is the AP state for each current scan. (b) Minor loop details: The current sweeps from the AP to the IS state and then back to the AP state. The transition from the IS to the P state is also shown. (c) Critical current as a function of net field for the AP to IS, IS to P, and IS to AP transitions for a 100×200 nm^2 pillar.

Because of the dipolar stray field (H_d) originating from the reference layer, the net field acting on the free layer is $H_{\text{net}} = H_a + H_d$, where H_a is the applied perpendicular field and $H_d \sim -200$ Oe. When a current of -7 mA is applied, we observe a strong reduction of the net switching field to ~ 0 Oe consistent with the efficient spin-torque reversal in films with perpendicular anisotropy [13]. In the present geometry, a negative current corresponds to electrons flowing from the reference to the free layer favoring the P state. A striking feature is that the reduction of the coercivity under a spin current is accompanied by the creation of an intermediate state (IS) that is characterized by an intermediate resistance. This state was not observed under the sole action of a magnetic field [14]. As illustrated in Fig. 1(c), the same IS can also be induced by increasing the negative current at constant field H_{net} from the initial AP state. The currents to create and annihilate such an IS for a given device are generally very reproducible.

The range of the IS in the I-H phase diagram is illustrated in Fig. 2(a). The initial magnetic configuration is the AP state, and the map has been realized by sweeping the negative current at constant magnetic field. We clearly observe that the IS is induced at a critical current value $I_{\text{AP}\to\text{IS}}$ for low magnetic fields ranging from $H_{\text{net}} \sim -200$ to 200 Oe. The observation of the IS even for $H_{\text{net}} = 0$ suggests that the current itself is able to create and stabilize this magnetic configuration. The IS stays stable up to a current $I_{\text{IS}\to\text{P}} > I_{\text{AP}\to\text{IS}}$ at which the P configuration is induced. By sweeping the current back after the creation of the IS, a positive current is found to restore the AP configuration at $I_{\text{IS}\to\text{AP}}$. This is shown in Fig. 2(b), where a minor loop of the current sweeps from the AP to the IS state and then back to the AP state at $I_{\text{IS}\to\text{AP}}$. Plotted in Fig. 2(c) is the variation of $I_{\text{AP}\to\text{IS}}$, $I_{\text{IS}\to\text{P}}$, and $I_{\text{IS}\to\text{AP}}$ vs H_{net} illustrating the field dependence and hysteretic behavior of the switching. It is clear that the IS can be manipulated in a controlled way and stabilized in zero current and field, and current can be used to restore either of the two uniform magnetization states.

An important feature illustrated in Fig. 2 is that the creation of the IS occurs only at small net fields H_{net} ranging from -200 to $+200$ Oe, which are typical values of DW pinning fields H_p in small elements, wires, and films with perpendicular anisotropy [1]. This along with the stability in zero field and current strongly suggests that the IS corresponds to a static DW state shown schematically in Fig. 3(a) rather than a steady dynamical mode [7]. In order to further investigate this assumption, we take advantage of this stable IS at $H = 0$ and $I = 0$ and measure the angular dependence of field required to go from the IS to the P configuration in Fig. 3(b). The angular behavior of the field required for the direct transition at $I = 0$ (without IS) is also plotted. The angular dependence of the AP $\rightarrow$ P transition is consistent with Stoner-Wohlfarth reversal of a uniaxial magnet. In contrast, the IS $\rightarrow$ P transition follows the $1/\cos(\theta)$ dependence expected for DW depinning processes, demonstrating that the IS corresponds to a stable DW. The fact that we observe only one IS and that the energy of Bloch DWs is large in such small elements suggests that this IS corresponds to a single DW with only one

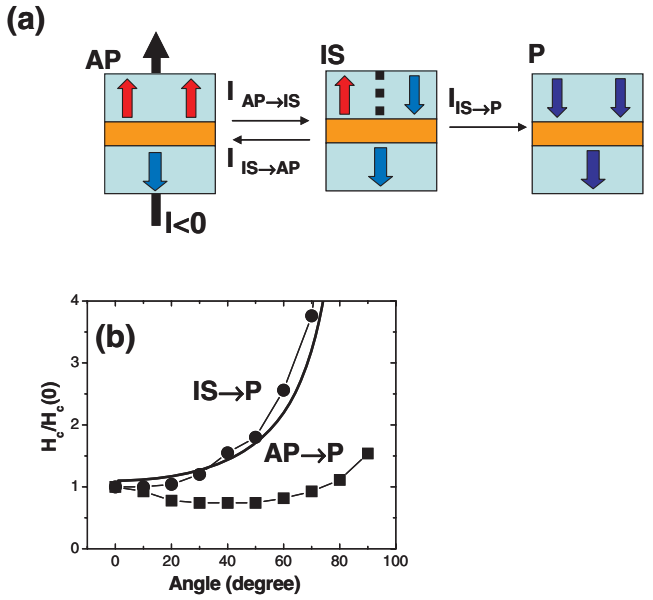

FIG. 3 (color). (a) Schematic illustration of the 3 different magnetic configurations (AP, IS, and P). The critical current corresponds to those described in Fig. 2(c). (b) Angular dependence of the switching field at $I = 0$ corresponding to the IS to P and AP to P transitions for a 100×200 nm^2 pillar. The IS at $I = 0$ has been prepared by using the procedure described in Fig. 2(b). The continuous line corresponds to the fit to the $1/\cos(\text{angle})$ law expected for DW propagation.

stable configuration. We estimate a DW width of $\sim$12 nm using a saturation magnetization of 650 emu/cm^3 and anisotropy $K_{\text{eff}} = 6 \times 10^6$ erg/cm^3 [13].

Patterned islands with perpendicular magnetic anisotropy are generally thought to reverse by Stoner-Wohlfarth behavior for diameters below $\sim$50–100 nm [15,16], where the magnetization is considered uniform (i.e., a macrospin). Above these dimensions, the islands are thought to reverse by nucleation of a low anisotropy volume (few tens of nanometers) at a nucleation field H_n. Since H_n is typically much larger than H_p of the DW, the entire island reverses at H_n. Under a spin-polarized current I, magnetization reversal can be initiated at fields $H_{nI} < H_n$ as seen in Fig. 1(a). In the limit where a small reversed domain nucleates at $H_{nI}(I) < H_p$, we might expect a DW state to be stabilized.

This assumption is consistent with micromagnetic simulations of the switching mechanism in our system at low magnetic fields using Landau-Lifshitz-Gilbert (LLG) equations of motion including the Slonczewski spin-torque term [13,17]. When increasing the negative current from the AP state, the free layer starts uniformly precessing with an increasing angle of precession until a small domain (typically on the edge of the sample) reverses. This reversed domain is damped while the opposite one keeps precessing under current. The free layer then subsequently reverses by DW motion, which is controlled, in part, by the presence of pinning sites. Indeed, the size of the resistance jump from the uniform to the IS state is slightly different (but always close to the halfway point) from nanopillar to nanopillar and reflects the relative areas of the up and down domains. We believe that this depends on the spatial location of the pinned DW that is determined by randomly distributed intrinsic and extrinsic pinning sites. In the future, it should be possible to engineer pinning sites to make this process more reproducible.

In order to check if a DW state could also be created in sub-100 nm elements for which a macrospin behavior is expected, we have used 50×100 nm nanopillars. Figure 4(a) clearly indicates the presence of a DW state at low applied fields when starting from the P state and sweeping the current positively (favoring an AP state). Figure 4(b) illustrates that this IS can also be manipulated to restore the two uniform magnetization states. However, we note that the creation of this IS is more stochastic than for the larger nanopillars. Also, once created, the DW state is very unstable, as illustrated by the strong field dependence of the $I_{\text{IS}\to\text{P}}$ transition and by the fact that the DW state configuration is not supported at both $H_{\text{net}} = 0$ and $I = 0$. These features are probably related to the high cost in energy to support a 12-nm wide Bloch DW in sub-100 nm elements.

Our demonstration of a current-induced DW state that cannot be created under a sole action of magnetic field has important implications from both a theoretical and a technological point of view. Even in very small nanoelements where a macrospin picture is expected, a DW state can be induced under current. The macrospin model can predict the onset of reversal where modeling suggests reversal initiates with uniform spin precession. However, as rever-

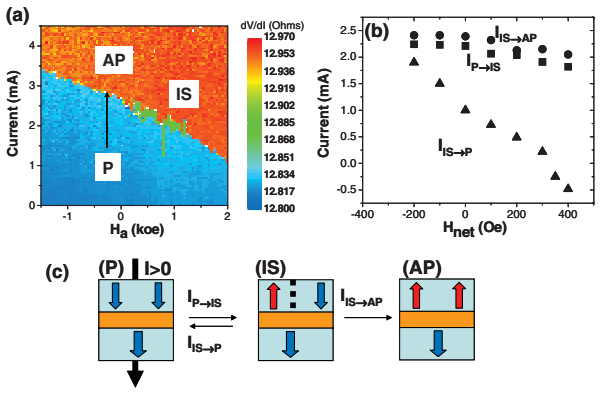

FIG. 4 (color). (a) Current-field phase diagram of dV/dI for a 50×100 nm pillar realized by measuring dV/dI while sweeping the current from 0 to 5 mA by steps of 50 μA at constant magnetic field H_a that is stepped by 50 Oe for each scan. The initial state is the P state for each current scan. (b) Critical current as a function of net field for the P to IS, IS to P, and IS to AP transitions for a 50×100 nm pillar. The critical currents have been obtained by averaging several measurements. (c) Schematic illustration of the 3 different magnetic configurations (AP, IS, and P). The critical currents correspond to those described in (b).

sal proceeds, the spin transfer mechanism allows nucleating and stabilizing a domain state by reducing the switching field of a nucleation volume below the pinning field. This result demonstrates that a spin current is able to destabilize locally a small volume of magnetization in agreement with the prediction that spin wave instabilities can be excited due to the presence of spatially nonuniform local fields [18]. Note that the IS has been found in all (about 6) the 100×50 and 100×200 nm^2 nanopillars that we have measured. However, it was present sometimes for a single branch and sometimes for both branches of the phase diagram ($P \rightarrow AP$ and $AP \rightarrow P$ transitions). This probably originates from a distribution of the magnetic properties of the nanopillars (dipolar and anisotropy fields, pinning defects, shape, etc.) that strongly influences the nucleation and propagation processes. Note also that, at temperatures <100 K, multi-DW states were found in larger pillars consistent with the thermally activated character of DW depinning process [1]. More generally, the presence of the DW state demonstrates that, even in such small structures, which typically are thought to reverse by coherent rotation, reversal by domain nucleation and propagation can also occur [15,16]. Depending on the sign of the applied field, the field may either support or oppose DW motion. As such, the detailed mechanism for spin-torque reversal with positive and negative applied fields may differ. Some indication of this can be seen in Figs. 2(c) and 4(b), where there is change in the slopes of $I_{\text{AP-P}}$ and $I_{\text{P-AP}}$ versus H_a on either side of the DW state where H_{net} changes sign.

Finally, we want to point out that other mechanisms may affect the switching and stabilization of this DW state under the action of currents. In this CPP configuration, there is no current torque acting on the Bloch DW itself, and it is not able to move it in the plane of the layers [1]. However, in a DW state, the current may be shunted into the domain of the free layer whose magnetization is parallel to the hard layer, decreasing the local current density flowing in the AP domain. This mechanism is likely to happen, since the local resistance difference between the P and AP channels is much higher than the total measured GMR which includes all the leads and layers resistances. This effect either stabilizes or destabilizes the DW state depending on the polarity of the current. A related mechanism is that, due to the presence of the DW state, the spin accumulation profile will be nonuniform across the device [19,20]. To our knowledge, the effects of nonuniform current distribution have not been explored in theoretical models.

In summary, we have demonstrated that magnetic nanopillars with perpendicular anisotropy exhibit stable intermediate domain states that can be accessed using spin-torque switching. This observation clearly shows that the macrospin model is not sufficient in these elements with perpendicular anisotropy even for nanopillars as small as 50×100 nm^2. The exact underlying effect of the spin transfer on this DW state creation and annihilation remains to be fully explained, with a particular emphasis on the influence of the DW state on the current flow. However, the ability to create and manipulate DW at low current densities in CPP nanopillars with strong coercivity could provide new prospects for ultrahigh density spintronic devices such as controlled DW nucleation in logic elements or multibit storage in nonvolatile memory cells. In this latter case, DW state could be stabilized in sub-50 nm nanoelements by using artificial pinning centers.

[1] See, for instance, D. Ravelosona, D. Lacour, J. A. Katine, B. D. Terris, and C. Chappert, Phys. Rev. Lett. **95**, 117203 (2005), and references therein.

[2] D. A. Allwood, G. Xiong, C. C. Faulkner, D. Atkinson, D. Petit, and R. P. Cowburn, Science **309**, 1688 (2005).

[3] Z. Li, J. He, and S. Zhang, J. Appl. Phys. **97**, 10C703 (2005).

[4] J. Shibata, G. Tatara, and H. Kohno, Phys. Rev. Lett. **94**, 076601 (2005).

[5] J. A. Katine, F. J. Albert, R. A. Buhrman, E. B. Myers, and D. C. Ralph, Phys. Rev. Lett. **84**, 3149 (2000).

[6] J. Grollier, V. Cros, A. Hamzic, J. M. George, H. Jaffres, A. Fert, G. Faini, J. Ben Youssef, and H. Legall, Appl. Phys. Lett. **78**, 3663 (2001).

[7] S. I. Kiselev *et al.*, Nature (London) **425**, 380 (2003).

[8] D. Chiba, Y. Sato, T. Kita, F. Matsukura, and H. Ohno, Phys. Rev. Lett. **93**, 216602 (2004).

[9] W. H. Rippard, M. R. Pufall, S. Kaka, S. E. Russek, and T. J. Silva, Phys. Rev. Lett. **92**, 027201 (2004).

[10] D. V. Berkov and N. L. Gorn, Phys. Rev. B **72**, 094401 (2005).

[11] J. Miltat, G. Albuquerque, A. Thiaville, and C. Vouille, J. Appl. Phys. **89**, 6982 (2001).

[12] J. Z. Sun, Phys. Rev. B **62**, 570 (2000).

[13] S. Mangin, D. Ravelosona, J. Katine, B. Terris, and E. E. Fullerton, Nat. Mater. **5**, 210 (2006).

[14] Note that, by using an ac field demagnetized procedure at $I = 0$, we were not able to obtain a multidomain ground state.

[15] G. Hu, T. Thomson, C. T. Rettner, S. Raoux, and B. D. Terris, J. Appl. Phys. **97**, 10J702 (2005); G. Hu, T. Thomson, C. T. Rettner, and B. D. Terris, IEEE Trans. Magn. **41**, 3589 (2005).

[16] J. Moritz, B. Dieny, J. P. Noziere, R. J. M. van de Veerdonk, T. M. Crawford, D. Weller, and S. Landis, Appl. Phys. Lett. **86**, 063512 (2005).

[17] LLG Micromagnetics Simulator, http://llgmicro.home.mindspring.com/.

[18] K. J. Lee, A. Deac, O. Redon, J. P. Nozieres, and B. Dieny, Nat. Mater. **3**, 877 (2004).

[19] J. Barnas, A. Fert, M. Gmitra, I. Weymann, and V. K. Dugaev, Phys. Rev. B **72**, 024426 (2005).

[20] B. Ozyilmaz, A. D. Kent, M. J. Rooks, and J. Sun, Phys. Rev. B **71**, 140403 (2005).